Thermochimica Acta, 229 (1993) 85–96
Elsevier Science Publishers B.V., Amsterdam

A new method of purity determination from the shape of fusion peaks of eutectic systems [1]

R.G. Bader, J.E.K. Schawe and G.W.H. Höhne *

Sektion für Kalorimetrie, Universität Ulm, D-89069 Ulm (Germany)

(Received and accepted 4 June 1993)

Abstract

A new method for purity determination of eutectic systems with the aid of differential scanning calorimetry (DSC) is described. This method allows the purity to be calculated directly from the form of the melting peak in the measured curve. The heating rate, sample mass and impurity are not restricted to small amounts.

INTRODUCTION

The form of melting peaks of impure substances depends on the impurity. In binary eutectic systems there are two components. Component 1 is the impurity and component 2 (the major component) is the pure substance. Component 1 melts completely at the eutectic temperature and component 2 in part due to the proportion at the eutectic point. Then the melting behaviour of the pure substance has to follow the liquidus curve.

Commercial methods for purity determination [1, 2] use the well known van't Hoff law. Use of this law restricts the method to very small impurities. Different methods are in use to eliminate the falsification of the measured curve; these are not theoretically well founded.

Another known method of purity determination uses an RC-model to simulate a measured DSC curve [3]. For this method it is necessary to adjust the purity as a parameter to fit the calculated curve to the measured one; a great amount of calculation is needed. Furthermore it is necessary to do other experiments to calculate the RC constants of the DSC model. The RC-model then only fits one special calorimeter so it cannot be used for any other instrument.

A disadvantage of both methods is the small heating rate which is necessary to obtain good results, because the smearing effect of the DSC must be kept small. In this paper a new method for purity determination is

---

* Corresponding author.

[1] Presented at the Tenth Ulm Conference, Ulm, Germany, 17–19 March 1993.

0040-6031/93/$06.00 © 1993 – Elsevier Science Publishers B.V. All rights reserved

presented, which takes the smearing into account and calculates the purity from the curve form. We start by describing the theoretical melting curve.

THEORETICAL CURVE FORM

The equilibrium between the pure solid component and liquid mixture obeys the condition of equal chemical potentials [4]. Because we discuss an ideal binary eutectic system, there is no necessity to consider excess quantities. This means the activity coefficients are equal to unity. The resulting equation is

$$\ln(x_2) = \frac{\Delta H_2}{R}\left(\frac{1}{T_2} - \frac{1}{T}\right) - \frac{\Delta C_{p2}}{R}\left(1 - \frac{T_2}{T} + \ln\frac{T_2}{T}\right) \qquad (1)$$

where $x_2 = 1 - x_1$ is the mol fraction in the mixture, ΔH_2 the enthalpy of fusion of the pure substances, ΔC_{p2} the difference of heat capacity in solid state and liquid state, T_2 the melting point of the component 2 and R the molar gas constant. Neglecting the temperature dependence of ΔH_2 implies that ΔC_{p2} is zero. Therefore we deduce

$$x_2(T) = e^{\frac{\Delta H_2}{R}\left(\frac{1}{T_2} - \frac{1}{T}\right)} \qquad (2)$$

These and further simplifications leading to van't Hoff's law are discussed with their total errors for different mixtures in ref. 5.

In Fig. 1 the liquidus curves of a eutectic system due to eqn. (2) are plotted. In the DSC experiment the heat flow rate is measured, so it is necessary to find the connection between the heat flow rate and the

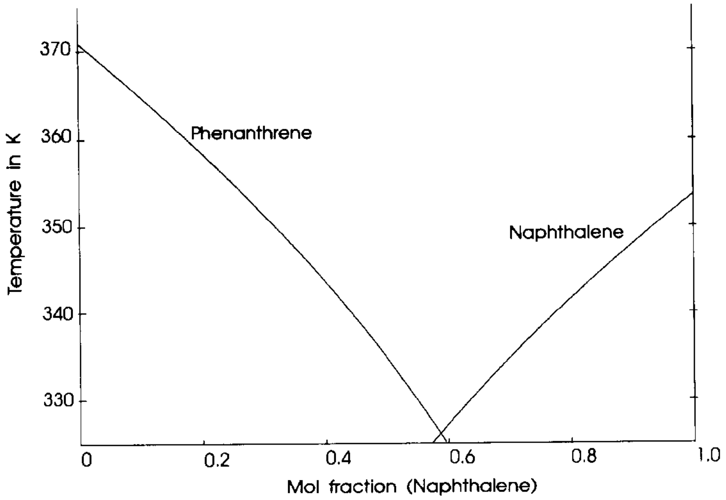

Fig. 1. Phase diagram of naphthalene ($\Delta H_2 = 18.549$ kJ mol^{-1}, $T_2 = 326.1$ K) and phenanthrene ($\Delta H_1 = 19.822$ kJ mol^{-1}, $T_1 = 370.9$ K).

temperature. The heat flow rate of a fusion peak $\Phi(t)$ is well known as

$$\Phi(t) = \frac{\partial Q_{\text{fus}}(T)}{\partial T}\frac{\partial T}{\partial t}$$

where Q_{fus} is the area (=heat) along the function $\Phi(t)$ up to the temperature T in question. The programme temperature changes linearly in time

$$T = T_0 + \beta t$$

where β is the heating rate and T_0 the start temperature. Therefore $\Phi(t)$ can be written

$$\Phi(t) = \frac{\partial Q_{\text{fus}}(T)}{\partial T}\beta$$

Usually the measured curve is plotted versus the temperature. We define

$$\varphi(T) = \frac{\partial Q_{\text{fus}}(T)}{\partial T} \tag{3}$$

Q_{fus} is related to the degree of crystallinity w_c of the mixture. Both quantities have a temperature dependency and the combining equation is

$$Q_{\text{fus}}(T) = (1 - w_c(T))Q_{\text{tot}} \tag{4}$$

where Q_{tot} is the total heat needed to fuse the mixture completely and $w_c(T)$ is the amount of solid that has not fused. In other words w_c has to be unity before the melting process and zero after its completion. At the eutectic point w_c has to be

$$w_c^{\text{eu}} = 1 - \left(x_{\text{imp}} + x_{\text{imp}}\frac{x_2(T_{\text{eu}})}{x_1(T_{\text{eu}})}\right)$$

where x_{imp} is the mol fraction of impurity, $x_1(T) = 1 - x_2(T)$ is the liquidus curve of component 1 and T_{eu} is the eutectic temperature. Setting $x_{\text{imp}} = 1 - x_{\text{pure}}$ and $x_1(T) = 1 - x_2(T)$ we obtain the temperature dependence of the degree of crystallinity $w_c(T)$ [6, 7]

$$w_c(T) = \frac{x_{\text{pure}} - x_2(T)}{1 - x_2(T)} \tag{5}$$

where x_{pure} is the mol fraction of the pure component. By combining eqns.

(2), (4) and (5) in eqn. (3) we are able to obtain a non-normalized theoretical melting peak.

It is necessary to normalize the theoretical function and likewise the measured peak to be able to compare them. We prefer a normalization due to the area equal to unity, to be sure of comparing the same energy amounts. Thus it is necessary to define the limits of integration. These are the eutectic temperature T_{eu} on the one hand and the end of fusion T_{end} on the other. The latter is easy to determine from eqn. (2)

$$T_{\text{end}}(x_{\text{pure}}) = \frac{\Delta H_2 T_2}{\Delta H_1 - \ln(x_{\text{pure}}) R T_2}$$

With the integration from eqn. (3) within the limits T_{eu} to T_{end} we obtain the normalization factor N. The normalized theoretical melting peak from eqns. (2)–(5) then reads

$$\varphi_{\text{norm}} = c_1 \frac{e^{c_1\left(\frac{1}{T_2}-\frac{1}{T}\right)}(x_{\text{pure}}-1)}{T^2\left[1-e^{c_1\left(\frac{1}{T_2}-\frac{1}{T}\right)}\right]^2\left[\dfrac{x_{\text{pure}}-1}{e^{c_1\frac{T_{\text{eu}}-T_2}{T_2 T_{\text{eu}}}}-1}-1\right]} \tag{6}$$

where the constant c_1 is defined as

$$c_1 = \frac{\Delta H_2}{R}$$

As a remark it should be mentioned that $\varphi_{\text{norm}} = \Phi_{\text{norm}}$, as the factor β is included in the normalization factor N.

Equation (6) is plotted for different purities in Fig. 2. Solving eqn. (6) for

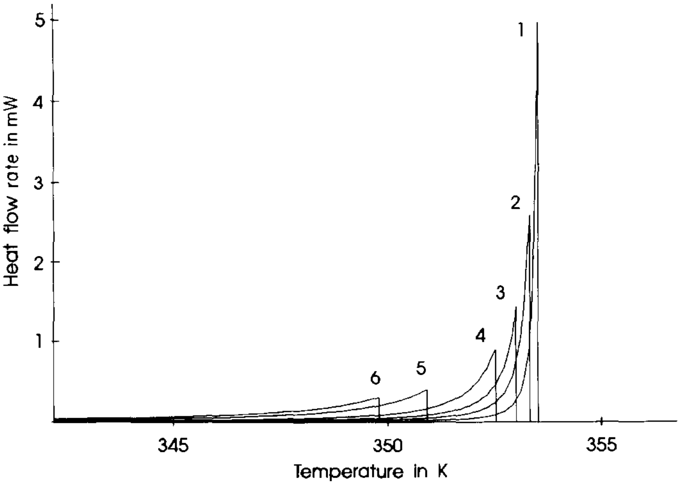

Fig. 2. Theoretical fusion peaks, normalized to unity area, with impurity levels: 1, 0.198%; 2, 0.553%; 3, 1.047%, 4, 2.029%; 5, 4.671%; 6, 6.646%.

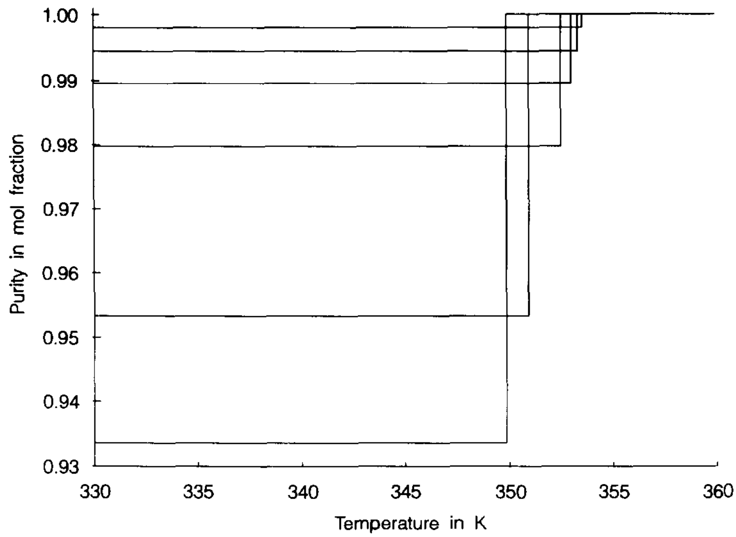

Fig. 3. Purity function of theoretical fusion peaks given in Fig. 2.

x_{pure} leads to

$$x_{\mathrm{pure}}(T,\varphi_{\mathrm{norm}}) = \frac{\varphi_{\mathrm{norm}}RT^2\left[\mathrm{e}^{c_1\frac{T_{\mathrm{eu}}-T_2}{T_2T_{\mathrm{eu}}}} - 2\mathrm{e}^{c_1\frac{2T_{\mathrm{eu}}T-T_{\mathrm{eu}}T_2-T_2T}{T_2TT_{\mathrm{eu}}}} + \mathrm{e}^{c_1\frac{3T_{\mathrm{eu}}T-2T_{\mathrm{eu}}T_2-T_2T}{T_2TT_{\mathrm{eu}}}}\right]}{\Delta H_2\left[\mathrm{e}^{c_1\frac{2T_{\mathrm{eu}}T-T_{\mathrm{eu}}T_2-T_2T}{T_2TT_{\mathrm{eu}}}} - \mathrm{e}^{c_1\frac{T-T_2}{T_2T}}\right] + \varphi_{\mathrm{norm}}RT^2\left[2\mathrm{e}^{c_1\frac{T-T_2}{T_2T}} - \mathrm{e}^{2c_1\frac{T-T_2}{T_2T}} - 1\right]} - \frac{\Delta H_2\left[\mathrm{e}^{c_1\frac{T-T_2}{T_2T}} - \mathrm{e}^{c_1\frac{2T_{\mathrm{eu}}T-T_{\mathrm{eu}}T_2-T_2T}{T_2TT_{\mathrm{eu}}}}\right]}{\Delta H_2\left[\mathrm{e}^{c_1\frac{2T_{\mathrm{eu}}T-T_{\mathrm{eu}}T_2-T_2T}{T_2TT_{\mathrm{eu}}}} - \mathrm{e}^{c_1\frac{T-T_2}{T_2T}}\right] + \varphi_{\mathrm{norm}}RT^2\left[2\mathrm{e}^{c_1\frac{T-T_2}{T_2T}} - \mathrm{e}^{2c_1\frac{T-T_2}{T_2T}} - 1\right]} \quad (7)$$

This function will be called the "purity function". The variables are T and φ_{norm}. All other parameters are constants.

Applying this equation to the theoretical curves in Fig. 2 we obtain Fig. 3 where the purity function is plotted versus the temperature. In a next step it is necessary to find eutectic system to compare the theoretical purity function form with the experimental one.

SAMPLE PREPARATION

In every eutectic system there is total miscibility of the components in the liquid phase, and no miscibility at all in the solid phases. However it is necessary to have a homogeneous sample in which every part of the solid body has the same proportion of the components.

We selected the components naphthalene with phenanthrene as impurity. First the components were weighed using 1 g of naphthalene and a matching mass of phenanthrene in the right proportion. Then the sample has to be mixed very carefully in the liquid state. To get a homogeneous mixture the sample was cooled down very quickly in ice water. That material was then powdered so it could be filled into the differential scanning calorimeter pans.

To test the homogeneity of the created mixture, several samples of equal masses from different parts of it were run in the differential scanning calorimeter, and then the different curves were compared. There were no differences in the normalized curves. The heating rate for all samples was 10 K min^{-1} and the sample mass was about 1 mg. In this way different mixtures were produced with different impurities from 0.198% to 6.646%.

PRACTICE FOR PURITY DETERMINATION

From the measured curves, baseline curves were subtracted (measured with same heating rate and an empty pan). These experimental curves have to be corrected with a second baseline to separate the heat of fusion from the heat flow due to the heat-capacity of the sample. This baseline starts at a point in front of the eutectic peak and ends at a point behind the fusion peak and is subtracted from the experimental curve.

The next step is the normalization of that experimental curve. For this purpose the curve has been integrated numerically. The area of interest is the melting region, so the integration limits are set to a point immediately behind the eutectic peak and to a point behind the end of fusion. This calculated area is then used to normalize the experimental curve.

With these corrected experimental curves (Fig. 4) a purity determination due to the purity function (eqn. (7)) can be done. The results are plotted in

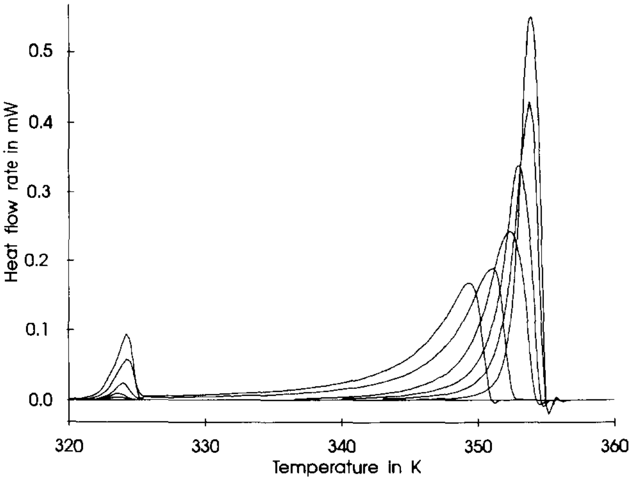

Fig. 4. Measured fusion peaks, normalized to unity area; impurities as in Fig. 2.

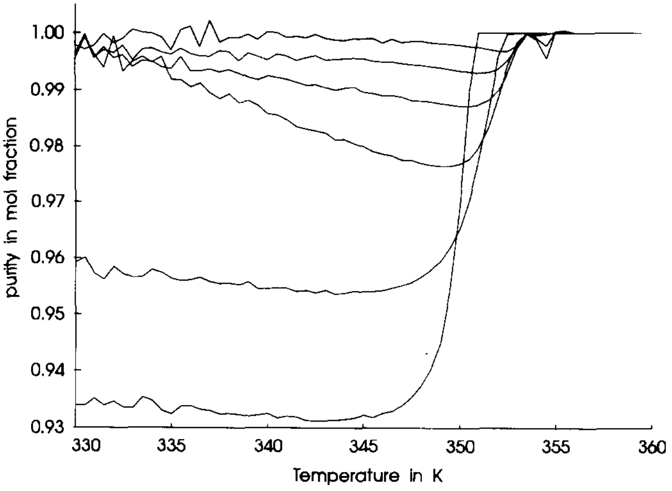

Fig. 5. Purity function of measured fusion peaks given in Fig. 4.

Fig. 5. It seems to be impossible to find the purity from these functions. The question arises as to how to come to curves similar to the theoretical curves (Fig. 3). As it is not allowed to change the curve form and use a form factor changing the area of the experimental curve, we have to look for a suitable method of correction.

To study the different influences of the function of the theoretical fusion, peak number 4 (Fig. 2) is used. There are some possibilities for a variation of parameters, namely the temperature shift, the measured heat flows and the measured enthalpy difference. These parameters also appear in eqn. (7).

The enthalpy variation must be allowed because the enthalpy is calculated from the DSC curve of the pure substance and depends on sample mass. The sample mass only can be weighed with an accuracy of ±0.05 mg. In our case with a sample mass of about 1 mg this leads to an uncertainty of the enthalpy of about 1 kJ mol^{-1}. The influence of this on the purity function form can be seen in Fig. 6. The function form itself does not change but the purity intersection moves. The effect is almost the same as changing the normalization factor, or multiplying the curve by a constant factor.

The next uncertainty is connected to the value of the measured heat flow rate. Usually it has an uncertainty of 1–3%. This uncertainty also appears in the measured baseline. The consequence of this is that the $\varphi_{\text{norm}}(T)$ values (as a difference) may be faulty by an unknown additive constant. To see this influence we added a constant of $\pm 1\ \mu$W to those $\varphi_{\text{norm}}(T)$ values from Fig. 2 with an impurity of 2.029% (peak 4). As can be seen in Fig. 7 the purity function changes in a very characteristic way.

The last quantity showing an uncertainty from measurement and which

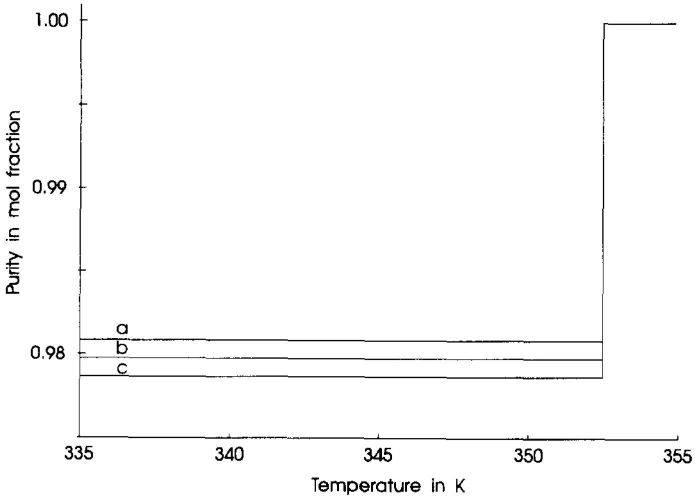

Fig. 6. Influence of enthalpy change on purity function of theoretical fusion peak no. 4 from Fig. 2; curve a, $\Delta H_{2\,\mathrm{meas}} - 1$ in kJ mol^{-1}; curve b, $\Delta H_{2\,\mathrm{meas}}$; curve c, $\Delta H_{2\,\mathrm{meas}} + 1$ in kJ mol^{-1}.

thus may be altered is the temperature. The calorimeter can only determine a temperature within the limits imposed by the calibration. The correction to obtain the true temperature depends on the heating rate and on the connection of the sample pan to the heater. Thus an additive constant to the detected temperature can be applied. In eqn. (2) the two temperatures T and T_2 appear only as a difference. The purity function (eqn. (7)) contains

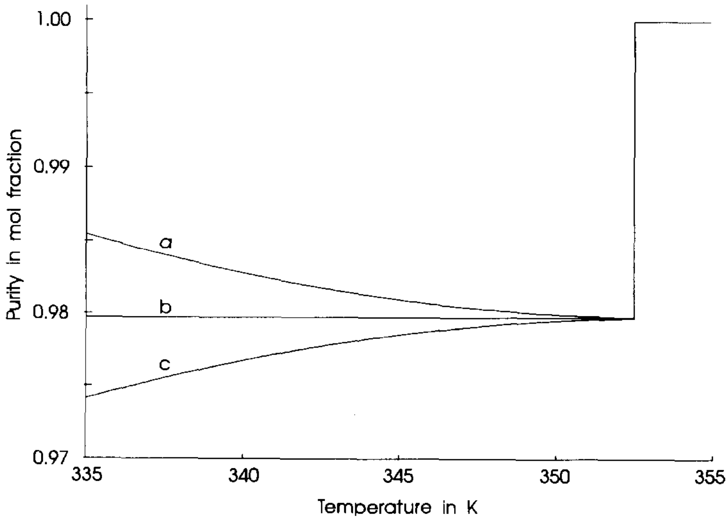

Fig. 7. Influence of variation of an additive constant on purity function of theoretical fusion peak no. 4 from Fig. 2; curve a, $\varphi_{\mathrm{norm,meas}}(T) - 1$ in μW; curve b, $\varphi_{\mathrm{norm,meas}}(T)$ in μW: curve c, $\varphi_{\mathrm{norm,meas}}(T) + 1$ in μW.

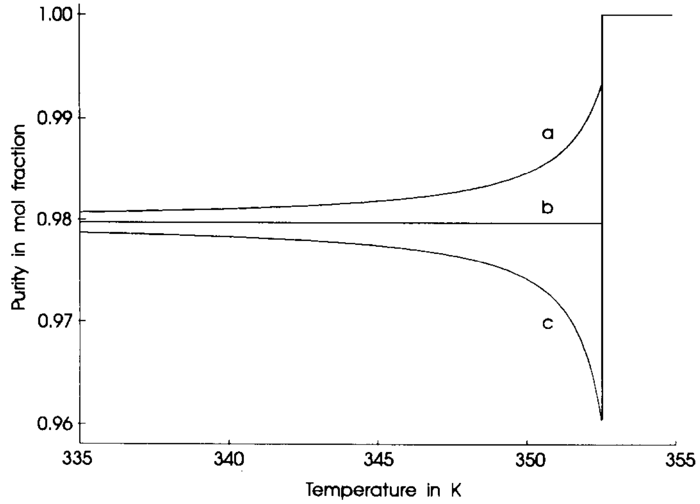

Fig. 8. Influence of variation of temperature T_2 on purity function of theoretical fusion peak no. 4 from Fig. 2: curve a, $T_{2\,\mathrm{meas}} - 0.5$ in K; curve b, $T_{2\,\mathrm{meas}}$ in K; curve c, $T_{2\,\mathrm{meas}} + 0.5$ in K.

eqn. (2) and obviously results in the same temperature dependence. As an additive constant correction of T leads to the same result as a correction of T_2, we restrict ourselves to varying T_2 (one value) instead of T (all measured values). In our case the temperature T_2 was changed by ±0.5 K. In Fig. 8 the influence of that change on the purity function is seen.

Assuming the heat flow rate and the temperature are measured slightly erroneously, a suitable change of T_2 and $\varphi_{\mathrm{norm}}(T)$, applied to the experimental curves in Fig. 4, should deliver (after purity calculation) a straight line parallel to the temperature axis. From the intersection of this straight line with the purity axis we then find the purity in question. The measured heat flow rates always scatter about the true value. To eliminate this noise for purity determination it is necessary to do some regression calculations. For the sake of simplicity we approximate the purity function by a straight line within certain limits. For the theoretical purity function the linear region for the purity determination is the eutectic temperature T_{eu} on the one side and T_{end} on the other.

In the case of obviously non-linear measured functions (Fig. 5) we have to choose the limits of linear regression individually. The experimental purity functions are linearized by variation of two parameters. The parameter changes are handled separately. We start with the temperature fit of T_2. As can be seen in Fig. 8, the greatest change of curve form due to the parameter change is near the step change on the right side. Therefore the limits for the linearization should be set near these points. In the case of the measured curve of 2.029% impurity, the limits were set to 347 K and 349 K. Within these limits we then calculated the linear regression line and changed the parameter T_2 until the slope of that line was below 10^{-8}. The corrected temperature T_2 is then used during the following fit of the heat flow rate values.

To find the correct additive constant for the heat flow rate correction, we consider the left side of the purity function because the influence of this parameter is greatest here. The greatest influence is indeed near the eutectic, but the experimental curve is very noisy there and it is better to start with the correction on the right of the noisy region. Some experience is necessary to find the proper limits for linear regression. It is recommended that the right side limit between those used for the temperature correction be chosen. We used 335 K and 343 K in our example. Otherwise the same procedure as for the temperature correction is applied to fit the second parameter.

It is very easy to write a computer program to linearize the purity functions of Fig. 5 by variation of the named parameters within the limits of accuracy of the measurement.

EXPERIMENTAL VERIFICATION

The experimental equipment used to measure the impurity curves (Fig. 4) was a Perkin-Elmer DSC 7 and a reconstructed DSC 2 with computer control [8]. The heating rate was 10 K $\min^{-1}$ and the sample masses were about 1 mg. The variations of $\varphi_{\text{norm}}(T)$ and T_2 were calculated for every sample with different impurities separately because of different heat conductivities and different measuring errors.

The results of our test measurements with prepared impurities, used corrections and calculated impurities both with our method and the commercial method (delivered with the DSC 7 evaluation software [1]) are listed in Table 1. The data of the experimental curves were transformed into an ASCII file. The following calculations were carried out on a PC 386 with the mathematical program MAPLE [9]. The computation time for purity

TABLE 1

Impurities and best fit parameters of different naphthalne samples

Prepared impurity in mol fraction $\times 10^2$	Parameter change T_2 in K	Parameter change φ_{norm} in μW	Determined impurity in mol fraction $\times 10^2$	Impurity usual method [1] in mol fraction $\times 10^2$
0.198	−0.609	0.4404	0.151	0.222
0.553	−0.782	0.2219	0.423	0.555
1.047	−0.423	0.9648	1.040	1.044
2.029	−0.487	2.5198	2.049	1.833
4.671	+0.595	1.5084	5.332	3.374
6.646	+0.318	1.1158	7.345	4.471

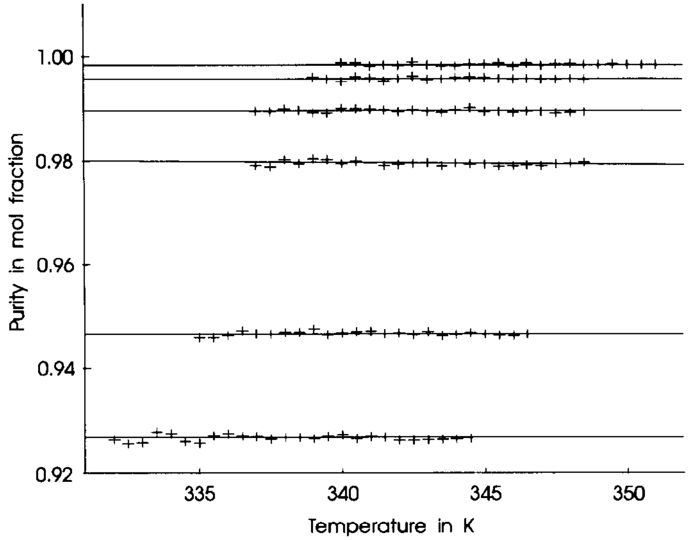

Fig. 9. Purity function of measured curves (Fig. 4) after linearization procedure. For parameter changes see Table 1, (+; corrected measured values, lines: linear regression).

determination of one sample varies from 20 to about 3 min depending on experience and noise of the measured curves. All program routines were written in the MAPLE macro language. The linear regression lines of the best fit are plotted in Fig. 9 together with measured values of our test materials. The limits of the linearization ranges in question can be seen from the range of measuring points visable in Fig. 9.

CONCLUSIONS

With the introduced method of purity determination it is possible to calculate the unknown purity directly from the curve form. It should be easily possible to integrate this method in DSC evaluation software.

Different measurements with variations of sample mass and variations of heating rates showed that large masses and large heating rates give the best results, because the noise of the heat flow then can be held at a minimum. This is an advantage over other methods. The curve form of a real measurement does not reassemble the theoretical one at all, but this does not matter because the introduced method works in that region of the transition peak where the curve smearing can be neglected or is compensated by the variations used.

REFERENCES

1 Perkin-Elmer Corporation, Determination of purity by differential scanning calorimetry, Thermal Analysis Newsletter No. 5, Norwalk, CT.
2 W.F. Hemminger and H.K. Cammenga, Methoden der Thermischen Analyse, Springer-Verlag, Berlin, 1989, p. 268 ff.

3 S. Sarge, S. Bauerecker and H.K. Cammenga, Thermochim. Acta, 129 (1988) 309.
4 R. Haase and H. Schönert, International Encyclopedia of Physical Chemistry and Chemical Physics 13/1, Solid–Liquid Equilibrium, Pergamon Press, Glasgow, 1969, p. 40.
5 S. Bauerecker, S.M. Sarge and H.K. Cammenga, J. Therm. Anal., 35 (1989) 527.
6 R.G. Bader, Diplomarbeit, Universität Ulm, Sektion Kalorimetie, 1993.
7 G.I. Asbach, Dissertation, Universität Ulm, Experimentelle Physik, 1972.
8 IfA GmbH, Schillerstraße 18, D-89077 Ulm, Hardware-Handbuch für DSC-2 Modernisierung, Ulm, 1992–1993.
9 MAPLE V, Waterloo Maple Software, University of Waterloo, Canada, 1981–1990.